Chemical Physics Letters 466 (2008) 50–55

Contents lists available at ScienceDirect

Chemical Physics Letters

journal homepage: www.elsevier.com/locate/cplett

# Circa conservation of vibrational energy among three strongly coupled modes of a cyanine dye molecule studied by quantum-beat spectroscopy with a 7 fs laser

Takayoshi Kobayashi [a,b,c,d,*], Ying Wang [a], Zhuan Wang [a,b], Izumi Iwakura [a,e]

[a] Department of Applied Physics and Chemistry and Institute of Laser Science, University of Electro-Communications, Chofugaoka 1-5-1, Chofu, Tokyo 182-8585, Japan
[b] JST, ICORP, Ultrashort Pulse Laser Project, 4-1-8 Honcho, Kawaguchi, Saitama 332-0012, Japan
[c] Institute of Laser Engineering, Osaka University, Yamadakami 2-6, Suita 565-0871, Ibaraki 567-0047, Japan
[d] Department of Electrophysics, National Chiao Tung University, 1001 Ta Hsueh Road, Hsinchu 3005, Taiwan
[e] JSPS Research Fellow, 8 Ichibancho, Chiyoda-ku, Tokyo 102-8472, Japan

ARTICLE INFO

*Article history:*
Received 5 April 2008
In final form 6 October 2008
Available online 11 October 2008

ABSTRACT

Real-time energy exchange among the three vibrational modes forming a triplet with frequencies $\omega_1$, $\omega_2$, and $\omega_3$ satisfying a 'circa sum-frequency relation', namely $\omega_1 + \omega_2 \cong \omega_3$ in a cyanine dye molecule has been studied with a 7-fs pulse laser. There are two triplets with average frequencies of the components of (146, 279, 432 $cm^{-1}$) and (279, 432, 738 $cm^{-1}$). Even though the circa sum-frequency relation is satisfied, circa-conservation of the vibrational energy holds among the three components only in the latter triplet. The difference between the two is ascribed to the symmetry of the molecular vibrational modes.


## 1. Introduction

Spectroscopy utilizing quantum beats was first applied for atomic systems to determine small energy spacings between neighboring sublevels utilizing the beat and its Fourier transform [1]. Quantum beats of large dye molecules in solution were observed using the technique of femtosecond transmission correlation [2]. These quantum beats were ascribed to interferences between coherently excited vibrational levels with beat frequencies corresponding to the energy spacing between the levels [3–5]. Extensions were made for molecular systems, which can be modeled by three-level schemes for determination of the electronic dephasing time [3,4,6].

Further applications have been developed for studies of the vibrational dynamics of multi-mode systems by pump–probe spectroscopy [1,3,4,6–19], in which the probe beam interrogates the non-stationary wave packets generated by the pumping. The pump-induced dynamics of absorption/emission as a function of delay time and probe wavelength reflects the temporal and spatial evolutions of these wave packets on the respective potential surfaces. Therefore, the use of time-resolved absorption spectra can be expected to determine the vibronic potential energy hypersurfaces on which the wave packet propagates [14].

The femtosecond pump–probe technique for studies of vibrational structures and dynamics in molecules has the following characteristic advantages over such conventional vibrational spectroscopy as spontaneous Raman scattering:

(1) Resonance Raman signals are frequently overwhelmed by fluorescence signals, especially for highly fluorescent molecules. In contrast, contamination by spontaneous fluorescence can be essentially avoided in real-time vibrational spectroscopy because the probe beam is much stronger and spatially coherent.
(2) Low-frequency modes, which are hardly detectable by Raman scattering due to intense Rayleigh scattering, can easily be studied by pump–probe spectroscopy as long as a few quanta of the modes can be covered within the laser spectral width with nearly constant phase.

Real-time spectroscopy is advantageous over time-resolved spontaneous, stimulated Raman spectroscopies and time-resolved infrared (IR) spectroscopy as follows:

(1) As a pure time-domain technique, the pump–probe method enables direct observation of vibronic dynamics including time-dependent instantaneous frequencies. Unlike conventional time-resolved vibrational spectroscopy, real-time spectroscopy enables detection of a very small change in frequency shifting nearly continuously in the real-time domain. This sensitive detection is realized by using a time step of 0.1 or 0.2 fs for the observation of absorbance changes and by the spectrogram method of a sliding window for the analysis. The width of the window is arbitrarily changeable depending on the required time resolution after obtaining experimental real-time data. The gate window can also be

* Corresponding author. Address: Department of Applied Physics and Chemistry and Institute of Laser Science, University of Electro-Communications, Chofugaoka1-5-1, Chofu, Tokyo 182-8585, Japan. Fax: +81 42 443 5825.
*E-mail addresses:* kobayashi@ils.uec.ac.jp (T. Kobayashi), wangying@ils.uec.ac.jp (Y. Wang).

0009-2614/$ - see front matter © 2008 Elsevier B.V. All rights reserved.
doi:10.1016/j.cplett.2008.10.015

modified to be probe-time-dependent. Therefore, the present technique can provide information on the structural changes of molecules even in transition states [20].

(2) Real-time spectroscopy can also provide information on the vibrational phase, which is inaccessible with conventional Raman and IR spectroscopy.

(3) The dynamics of vibrational modes coupled with the electronic transition can be studied in relation to the decay dynamics of the electronic excited states by simultaneously using the same measurement system under exactly identical experimental conditions such as laser power, temperature, and probing sensitivity.

In spite of these overwhelming advantages of the femtosecond pump–probe experiment, the assignment of the pump–probe signals to either the ground state or the electronic excited state(s) remains ambiguous. This is because an ultrashort laser pulse with a wide enough spectrum can drive coherent vibrations in the ground state and in one or more excited states by the generation of superposed vibrational levels in both states. This hinders a clear-cut discussion on the dynamics of the wave packets after photogeneration.

In the present study, we have applied the ideas mentioned above to an analysis of the nature of mode coupling among the vibronic modes of a cyanine dye molecule, 1,1′,3,3,3′,3′-hexamethyl-4,4′,5,5′-dibenzo-2,2′-indotricarbocyanine (HDITC). The ultrafast dynamics in solution of this molecule and a similar cyanine dye, 1,1′,3,3,3′,3′-hexamethyl-2,2′-indotricarbocyanine iodide (HITC), have been studied in some detail by photon echo measurements [21,22] and pump–probe spectroscopy [23–27].

We report here on the mode coupling among the vibronically coupled three modes in HDITC in ethanol solution, where we have observed circa energy conservation in two specific groups of three modes among 237 modes, however only in one of the two a mode coupling is taking place according to the calculation in the present paper.

## 2. Experimental and calculation methods

### 2.1. Instrumentation

Pump-and-probe light sources were taken from a non-collinear parametric amplifier (NOPA) [28–31]. The pulse duration from NOPA was 6.8 fs for FT-limited pulses by calculating from the laser spectrum, which covered a range of 556−753 nm, and 7.1 fs by the auto-correlation measurement.

A multichannel lock-in amplifier was used in this experiment to detect the pump–probe signals. The signals were spectrally resolved using a polychromator (JASCO, M25-TP) at 128 wavelengths from 556 to 753 nm and were detected by avalanche photodiodes. Lock-in amplifiers were used with a reference from an optical chopper modulating the pump pulse intensity at 2.5 kHz.

### 2.2. Sample materials

Cyanine dye HDITC (Exciton) was used without further purification. It was dissolved in ethanol (Kanto Kagaku, special grade), and had an optical density of 1.2 at 720 nm in a 1 mm thick quartz cell.

### 2.3. Quantum chemical calculation

The unrestricted Becke three-parameter hybrid exchange functional combined with the Lee–Yang–Parr correlation functional (B3LYP) [32,33] was used with the 6-31+G* basis sets for geometry optimizations and vibrational analyses. As for the d orbital, 5d functions were used. The quantum chemical calculations were performed using the GAUSSIAN 03 program package [34] without assuming symmetry. It was confirmed that all the frequencies were real.

## 3. Results and discussion

### 3.1. Analysis of vibrational modes

The traces of the delay time dependence of the normalized difference transmittance, $\Delta T(t)/T$, induced by an ultrashort pump pulse were used to calculate the absorbance change, $\Delta A(t)$. This trace is called a 'real-time spectrum', because it is a spectrum in the time domain instead of the frequency domain for conventional spectroscopy.

Fig. 1a shows the real-time traces measured at eight different photon energies. These oscillations arise from molecular vibration, which is coupled with the electronic transition that modifies the instantaneous absorbance change $\Delta A(t)$ at delay time $t$ probed at

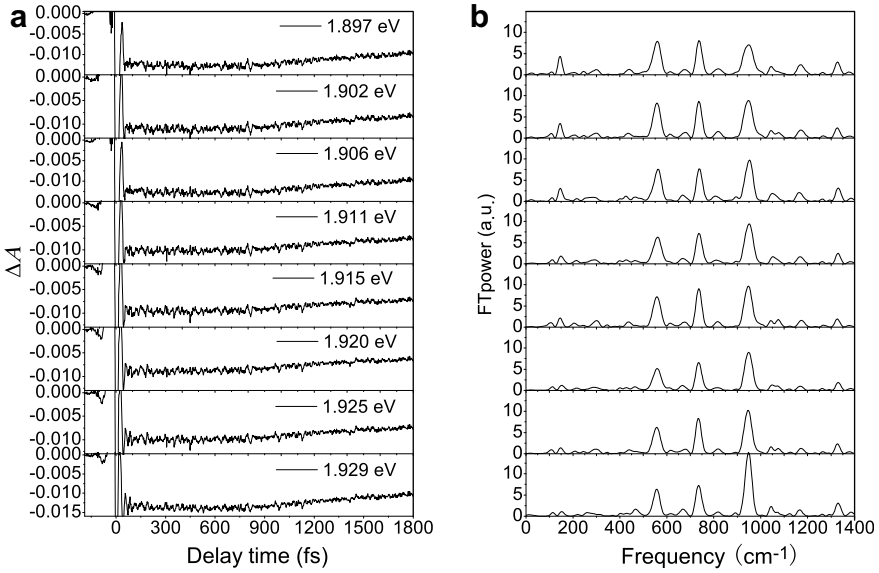


**Fig. 1.** (a) Real-time absorbance changes at eight probe photon energies; (b) FT power spectra of the traces in (a).

each wavelength. This results in a change in the spectral shape within the period of molecular vibration.

FT power spectra, shown in Fig. 1b, were calculated to detect the frequency components of the vibration. They have eleven strong peaks at 146, 279, 432, 561, 738, 944, 1050, 1172, and 1330 $cm^{-1}$. All modes except 1172 $cm^{-1}$ had been observed by a pump–probe spectrum, which had the center wavelength at 800 nm [27] at 135, 297, 436, 575, 730, 936, 1057, and 1310 $cm^{-1}$, i.e., with smaller differences than 20 $cm^{-1}$. In the present Letter, we denote 'spatial frequency' as 'frequency' and use it in units of $cm^{-1}$.

In the probe photon energy (wavelength) ranging 1.88–2.00 eV (660–620 nm), the probe light was more intense than in other ranges, and hence it enabled the observation of $\Delta A(t)$ signals with a higher signal-to-noise ratio than in the other ranges. Therefore, we mainly focus here on the vibrations observed in the probe photon energy ranging between 1.88 and 2.00 eV. Fig. 2 shows the two-dimensional (2D) Fourier power spectra against the probe photon energy and wavelength.

The ultrashort pulse, which is resonant with a transition to an electronic excited state, can be coupled with various vibrational modes with two or more vibrational levels in each mode that compose vibrational wave packets. The origin of the wave packet motion can therefore be identified from the phase of the vibrational oscillation obtained from the Fourier transform of the real-time trace. The vibrational amplitude $V(t)$ of a single mode vibration is given by

$$V(t) = V(0)\cos(\omega_v t + \phi) \quad (1)$$

Here $V(0)\cos\phi$ is the initial amplitude, $\omega_v$ is the vibrational frequency, and $\phi$ is the vibrational phase, which is expected to be $\pi/2$ and $\pi$, respectively [35]. The phases of four modes, a–d probed at 1.91 eV (650 nm) with frequencies at $\omega_a = 146\ cm^{-1}$, $\omega_b = 279\ cm^{-1}$, $\omega_c = 432\ cm^{-1}$, and $\omega_d = 738\ cm^{-1}$ were determined as $\phi_a = 0.88\pi$, $\phi_b = 0.05\pi$, $\phi = -0.09\pi$, and $\phi_d = 0.90\pi$. Therefore, all of them are mainly assigned dominantly to the wave packet motion in the excited state.

### 3.2. Analysis of time-dependent frequency and energy by spectrograms

We have selected the following two groups from the four modes: Group 1 (G1): ($\omega_a$, $\omega_b$, $\omega_c$), and Group 2 (G2): ($\omega_b$, $\omega_c$, $\omega_d$), which approximately satisfy the sum–frequency relations $\omega_1 + \omega_2 \cong \omega_3$. The symbols $\omega_a$, $\omega_b$, $\omega_c$ for G1 and $\omega_b$, $\omega_c$, $\omega_d$ for G2 correspond to $\omega_1$, $\omega_2$, and $\omega_3$, respectively. This sum-frequency relation may be accidental, but a characteristic feature can be extracted from the time dependence and the correlation among the 'instantaneous' frequencies of the modes.

G1 is first taken up as a basal unit for our subsequent discussion. The sum of the mean frequencies of the two modes in G1, $\omega_a + \omega_b \sim 425\ cm^{-1}$, deviates from $\omega_c \sim 432\ cm^{-1}$ by $\sim 7\ cm^{-1}$. In the case of G1, energy conservation seems to be satisfied where two vibrational quanta from each of the two modes, $\omega_b$ and $\omega_c$, are destroyed and one quantum of mode, $\omega_a$, is generated. A similar situation is also expected for G2, in which $\omega_b$ and $\omega_c$ are destroyed and one quantum of mode, $\omega_d$, is generated. As can be seen from the following discussion, however, the two triplets behave in totally different ways.

To study the time course of the matching condition, we have utilized the spectrogram method. It can provide time-dependent energy conservation among the three corresponding vibrational modes.

The spectrograms were calculated for the real-time traces probed in this specific spectral range, where the result for the probe photon energy of 1.91 eV (650 nm) is shown as an example in Fig. 3 in the form of a 2D contour map of $\Delta T(t)$ against the gate delay and the instantaneous frequency. The time gating of the spectrogram was calculated using a Blackman-type window function with a half width at half maximum (HWHM) of 200 fs, which corresponds to the Fourier width of $\sim 31\ cm^{-1}$ in the Blackman window. The frequency separations of the adjacent mode of 146, 279, 432, and 738 $cm^{-1}$ are 133, 153, and 306 $cm^{-1}$, respectively; all of them substantially exceed 31 $cm^{-1}$. Therefore, the interference effects among the relevant modes can be ignored in the spectrogram analysis. In addition, the frequency must match the period of vibration, which is equal to the inverse of the frequency difference, if any interference were to take place. However, the observed highly aperiodic frequency modulation cannot be explained in terms of such interference.

Let us discuss here the importance of the time-dependent frequencies obtained in the spectrogram. When a medium or a large molecule is excited by an ultrashort pulse radiation, wave packets of several modes are generally created after excitation. The wave

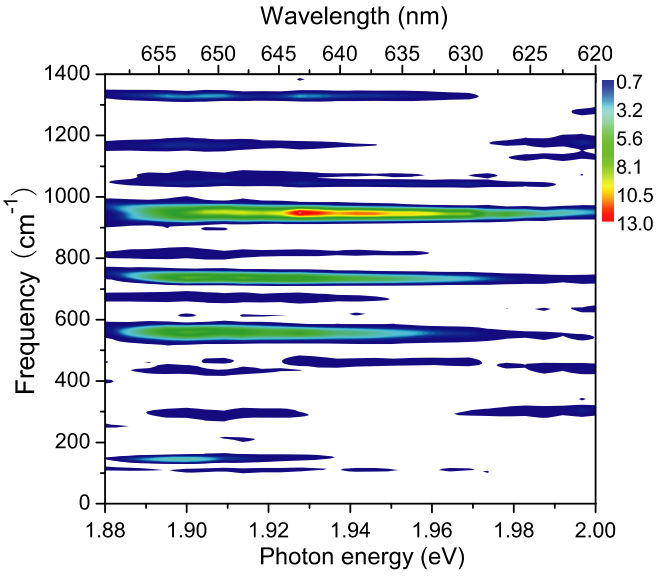


**Fig. 2.** The 2D FT power of the photon energy range from 1.88 to 2.00 eV.

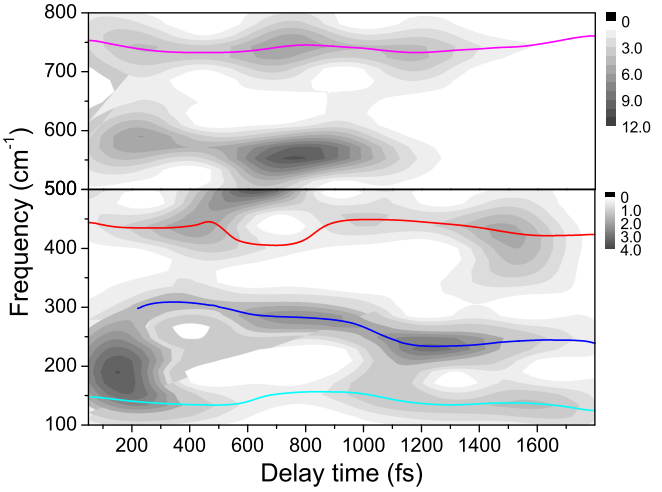


**Fig. 3.** Spectrogram of 650 nm using a Blackman window with 200 fs HWHM. Ranges of 100–500 and 500–800 $cm^{-1}$ are shown in the contour map scale displayed in the intensity bars on the right side. Colored curves are the peak traces of frequencies for modes $\omega_a = 146\ cm^{-1}$, $\omega_b = 279\ cm^{-1}$, $\omega_c = 432\ cm^{-1}$, and $\omega_d = 738\ cm^{-1}$.

functions of these wave packets are linear combinations of eigenstates with more than one vibrational quantum number ($v = v_1, \ldots, v_n$) being covered by the laser pulse spectrum (under the assumption that it is Fourier transform limited). Then the coherent vibrational energy transfer and subsequent ones take place as time evolves. In the former coherent transfer process, the initially created coherences in modes are changed into those of different vibrational modes through mode coupling. Finally, the coherences are dissipated resulting in a random phase state.

The peak traces of the frequencies for the four modes are drawn by colored curves in Fig. 3. The traces of instantaneous frequencies $\omega_i(t)$ ($i = a–d$) and instantaneous vibrational intensities $n_i(t)$ of each mode were obtained from this figure, and the signals at different delay times were fitted by fifth-order polynomials. The peak traces of each mode, drawn by connecting the peak points at different delay times, are shown in Fig. 4a and b.

### 3.3. Circa conservation of vibrational energy

From the corresponding principle between quantum mechanics and classical dynamics, the instantaneous power of the molecular vibration, which is proportional to the squared amplitude of the coordinate displacement from equilibrium, can be assumed to be proportional to the vibrational quantum number if the effect of zero point energy is ignored. To obtain the vibrational energy, the instantaneous vibrational amplitudes multiplied by the instantaneous frequencies of the $n_i(t)\omega_i(t)$ for the four modes a–d are plotted against the delay time $t$ in Fig. 4c.

The instantaneous sum–frequency relations ($\omega_3 - \omega_1 - \omega_2 = 0$) of two groups are shown in Fig. 4d, and the instantaneous energy conservation ($n_1(t)\omega_1(t) + n_2(t)\omega_2(t) + n_3(t)\omega_3(t) = \text{constant}$) of each corresponding group is shown in Fig. 4e. Although the vacuum energies are not included in the relation, $(1/2)\omega_1(t) + (1/2)\omega_2(t) = (1/2)\omega_3(t)$ is also satisfied as well, and hence the above discussion is rationalized equally well.

For a detailed analysis of the four modes in G1 and G2 and the relationship between them, we list the mean values of the frequency, intensity, and their standard deviations of each frequency, and intensities for each mode in Table 1. We calculated the standard deviation of instantaneous frequency mismatch of each group in this time range from those derived from Fig. 4d. We also calculated the degrees of energy mismatch for each mode and for the sum of the energy of the three members of the mode in each group as listed in Table 1. If we assume that the fluctuations of modes of G1 are completely random, then the amount of the fluctuation can be calculated to be 23% of the average total energy in the triplet. This is nearly equal to the fluctuation of the observed 25% total energy in G1. Totally different features can be observed for G2. The fluctuation of the total energy in this group, which amounts to 14% of the average total energy, is much larger than the observed fluctuation of 9%. This indicates that the coupling among the three in G2 is strong and that the energy is approximately conserved within the group. The difference in such energy conservation can thus reveal the conversation of the energy fluctuations of vibrational modes and provide information on the coupling strengths.

### 3.4. Comparison of symmetry relations among the modes between the two groups

The matching of the circa sum relation of average frequencies, $\omega_1 + \omega_2 \cong \omega_3$, is better satisfied in G1 than in G2. However, the situations of the two groups are totally different from this relation, as

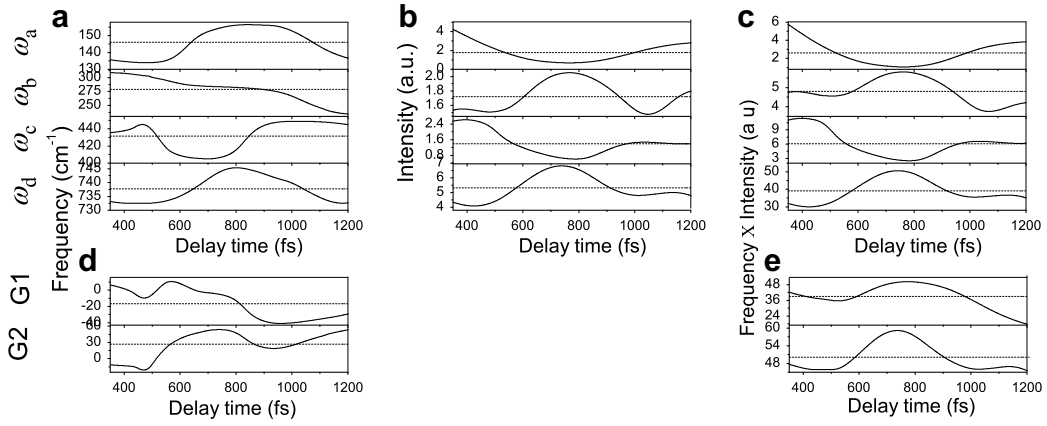


**Fig. 4.** (a) Instantaneous vibrational frequencies of four modes: 146, 279, 432, and 738 cm$^{-1}$ from 350 to 1200 fs; (b) instantaneous vibrational intensities of (a); (c) instantaneous vibrational frequency multiplied by the instantaneous vibrational intensity of each mode; (d) mismatch of instantaneous vibrational amplitudes $\omega_3 - \omega_2 - \omega_1$ of the two groups listed in Table 1; (e) mismatch $\omega_3 - \omega_2 - \omega_1$ of the two groups listed in Table 1. The dashed line in each figure is the instantaneous mean value of the peak vibrational frequency of each contour component across the frequency distribution.

**Table 1**
Mean frequencies and intensities and their standard deviations (SD) of the four modes in the range of 350–1200 fs delay time.

| Mode | Frequency (cm$^{-1}$) | | Intensity (a.u.) | | Energy (a.u.) | | Coupled modes in each triplet | |
|---|---|---|---|---|---|---|---|---|
| | Mean value | SD | Mean value | SD | Mean value | SD | 1 | 2 |
| $\omega_a$ | 146 | 9 (6.0%) | 1.78 | 0.9 (52.5%) | 2.53 | 1.22 (48.3%) | * | |
| $\omega_b$ | 279 | 21 (7.5%) | 1.72 | 0.2 (11.4%) | 4.81 | 0.64 (13.4%) | * | * |
| $\omega_c$ | 432 | 17 (3.9%) | 1.39 | 0.6 (43.2%) | 6.06 | 2.71 (44.7%) | * | * |
| $\omega_d$ | 738 | 5 (0.6%) | 5.31 | 0.9 (16.1%) | 39.22 | 6.52 (16.6%) | | * |
| Mismatch of mean frequency $\lvert\omega_3–\omega_2–\omega_1\rvert$ (cm$^{-1}$) | | | | | | | 7 | 27 |
| SD of instantaneous frequency mismatch (cm$^{-1}$) | | | | | | | 32 | 23 |
| Fraction of energy mismatch | | | | | | | 25% | 9% |

* Show the members of each group.

mentioned in the previous subsection. The difference can be ascribed to the symmetry of the molecular vibrational modes, as discussed in the following.

The displacement of atoms in the vibrational modes in HIDTC molecule with frequencies is close to those of the modes being studied. We calculated the frequencies of 136, 138, 149, 283, 304, 308, 422, 734, and 738 $cm^{-1}$. The frequencies of 136, 138, and 149 $cm^{-1}$ are close to $\omega_a = 146\ cm^{-1}$ and those of 283, 304, and 308 $cm^{-1}$ are close to $\omega_b = 279\ cm^{-1}$. The frequency of 422 $cm^{-1}$ is close to $\omega_c = 432\ cm^{-1}$ and those of 734 and 738 $cm^{-1}$ are close to $\omega_b = 734\ cm^{-1}$.

The displacements of atoms in the modes of 138, 283, 422, and 734 $cm^{-1}$ are shown in Fig. 5 as examples. It is difficult to assign the four observed modes. However, because 136, 138, and 149 $cm^{-1}$ are all close enough to $\omega_a = 146\ cm^{-1}$, they are likely to be mixed in the observed mode of 146 $cm^{-1}$. A similar discussion can be made for 283, 304, and 308 $cm^{-1}$ and 734 $cm^{-1}$. Even if the modes of $\omega_a$ and $\omega_b$ are not uniquely assigned among the candidates, the following symmetry discussion should still be valid.

Among the modes discussed above, the modes of 136, 138, 149 $cm^{-1}$ (candidates of $\omega_a$) and 422 $cm^{-1}$ (candidate of $\omega_c$) can be classified into the $C_{2v}$ point group symmetry of a simplex group of A1, as shown in Fig. 5a. However, the others, 283, 304, and 308 $cm^{-1}$ (candidates of $\omega_b$) and 734 $cm^{-1}$ (candidate of $\omega_d$) cannot be clearly classified either to a simplex group of any type because of the deviation of the symmetry of the molecule from $C_{2v}$.

Here we would like to discuss the coupling among the three modes, of which the amplitudes are described as follows:

$$Q_i = q_i \exp[\mathrm{i}(\omega_i t + \phi_i)] + \mathrm{c}\cdot\mathrm{c}. \quad i = 1,2,3 \tag{2}$$

It is assumed that the frequency relation $\omega_1 + \omega_2 = \omega_3$ is satisfied among the three modes. Then the equations of motions of the three modes with complex amplitudes of $q_1$, $q_2$, and $q_3$ are given by the following three coupled equations, using the coupling constants $u_{12}$, $u_{23}$ and $u_{31}$ as follows:

$$-\frac{\partial q_1}{\partial t} = \frac{1}{\tau_1} q_1 - u_{23} q_2^* q_3 \tag{3}$$

$$-\frac{\partial q_2}{\partial t} = \frac{1}{\tau_2} q_2 - u_{31} q_3 q_1^* \tag{4}$$

$$-\frac{\partial q_3}{\partial t} = \frac{1}{\tau_3} q_3 - u_{12} q_1 q_2 \tag{5}$$

Here $\tau_1$, $\tau_2$ and $\tau_3$ are the dephasing times of corresponding modes. From Eq. (5), $q_3$ can be obtained as follows:

$$q_3(x,y,z,t) = \int_{-\infty}^{t} \exp\left(-\frac{t-t'}{\tau_3}\right) u_{12} q_1(x,y,z,t') q_2(x,y,z,t')\mathrm{d}t' \tag{6}$$

Here we assume that $q_1$ and $q_3$ have a mirror symmetry while $q_1$ does not.

We operate the minor operator $M$ to $q_1$, $q_2$ and $q_3$

$$Mq_1(x,y,z,t) = q_1(x,y,-z,t) = q_1(x,y,z,t) \tag{7}$$

$$Mq_2(x,y,z,t) = q_2(x,y,-z,t) \neq q_2(x,y,z,t) \tag{8}$$

$$Mq_3(x,y,z,t) = q_3(x,y,-z,t) = q_3(x,y,z,t) \tag{9}$$

We operate $M$ to both right-hand and left-hand sides of Eq. (6):

$$\begin{aligned} Mq_3(x,y,z,t) &= \int_{-\infty}^{t} \exp\left(-\frac{t-t'}{\tau_3}\right) Mu_{12} q_1(x,y,z,t') q_2(x,y,z,t')\mathrm{d}t' \\ &= \int_{-\infty}^{t} \exp\left(-\frac{t-t'}{\tau_3}\right) u_{12} q_1(x,y,z,t') q_2'(x,y,z,t')\mathrm{d}t' \\ &= q_3(x,y,z,t) \\ &= \int_{-\infty}^{t} \exp\left(-\frac{t-t'}{\tau_3}\right) u_{12} q_1(x,y,z,t') q_2(x,y,z,t')\mathrm{d}t' \end{aligned} \tag{10}$$

where $q_2(x,y,z,t) \neq q_2'(x,y,z,t)$.

This is satisfied only when $u_{12} = 0$. Therefore, this mode cannot couple the other two modes even if they satisfy the energy conservation law.

According to the aforementioned theory, $\omega_a$ and $\omega_b$ in the present case cannot couple each other to create $\omega_c$ because of symmetry even if the frequency matching is satisfied, while $\omega_b$, $\omega_c$, and $\omega_d$ do not have this kind of relationship, $\omega_b$ and $\omega_c$ have the possibility to couple and create $\omega_d$.

### 3.5. Condition for the formation of a triplet satisfying circa energy conservation

Though the ultimate goal of a vibrational spectroscopic analysis is a complete assignment of observed vibrational signals, it is rarely possible for such a complicated molecule as that studied in the present Letter. It is especially difficult to achieve trustable mode assignments, because all the modes discussed above belong to excited state wave packets.

As shown in this Letter, the coupling strength among the three modes $\omega_1$, $\omega_2$, and $\omega_3$, can be estimated from the comparison of fluctuations of instantaneous frequencies and that of total energy. Therefore, the present method of circa conservation of vibrational modes is expected to provide a valuable guide for a spectral analysis by evaluation of the mode coupling strength even without mode assignment. Furthermore, the degree of vibrational energy conservation as an indicator of coupling strength may also be useful for the mode assignment by consideration of symmetry. The example of this is shown in this Letter. The coupling strength between the modes with the same symmetry is expected to be much

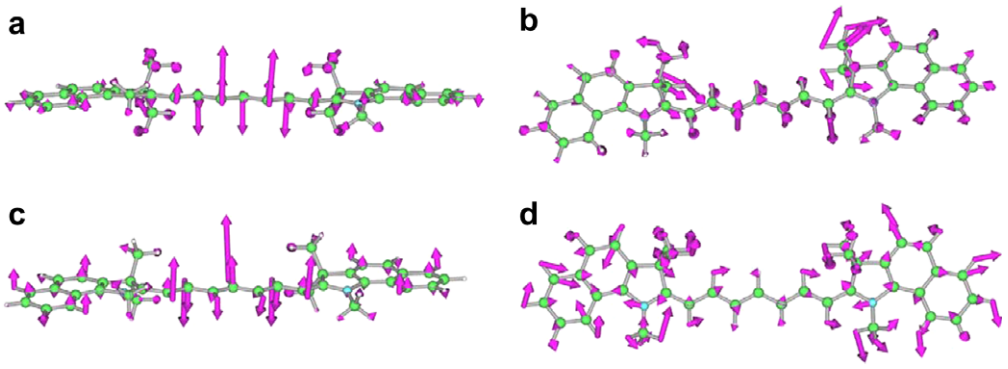


**Fig. 5.** The displacement of atoms on the vibrational modes in molecule HDITC with frequencies of (a) 138 $cm^{-1}$; (b) 283 $cm^{-1}$; (c) 422 $cm^{-1}$ and (d) 734 $cm^{-1}$.

higher than those without the same symmetry, as clearly shown in this Letter.

## 4. Conclusion

Real-time energy exchange among the three coupled vibrational modes in a cyanine dye molecule has been studied by using a duration pulse laser with a few optical-cycles having a visible to near-IR spectrum. An analysis of the delay time dependence of the intensities among the three modes in the triplet of (279, 432, 738 $cm^{-1}$) has provided the first experimental verification of the circa conservation of the vibrational energy for each of the three modes in the triplet, (146, 279, 432 $cm^{-1}$), where the energy fluctuation has been verified to be completely random. The present study shows that an analysis of the degree of energy conservation can be used as an index of the coupling strength among the vibrational modes.

## Acknowledgments

This work was partly supported by a 21st Century COE program on 'Coherent Optical Science' and partly supported by a grant from the Ministry of Education (MOE) in Taiwan under the ATU Program at National Chiao Tung University. A part of this work was performed under the joint research project of Laser Engineering, Osaka University, Under Contract subject B1-27.

The authors are grateful to the Information Technology Center of the University of Electro-Communications for their support of the DFT calculations. This work was supported by Grant-in-Aid for JSPS Fellows to I.I.

## References

[1] J. Mlynek, W. Lange, Opt. Commun. 30 (1979) 337.
[2] M.J. Rosker, F.W. Wise, C.L. Tang, Phys. Rev. Lett. 57 (1986) 321.
[3] I.A. Walmsley, M. Mitsunaga, C.L. Tang, Phys. Rev. A 38 (1988) 4681.
[4] I.A. Walmsley, C.L. Tang, J. Chem. Phys. 92 (1990) 1568.
[5] I.A. Walmsley, F.W. Wise, C.L. Tang, Chem. Phys. Lett. 154 (1989) 315.
[6] F.W. Wise, M.J. Rosker, C.L. Tang, J. Chem. Phys. 86 (1987) 2827.
[7] G. Cerullo, G. Lanzani, M. Muccini, C. Taliani, S. De Silvestri, Phys. Rev. Lett. 83 (1999) 231.
[8] T. Kobayashi, A. Shirakawa, H. Matsuzawa, H. Nakanishi, Chem. Phys. Lett. 321 (2000) 385.
[9] A. Sugita, T. Saito, H. Kano, M. Yamashita, T. Kobayashi, Phys. Rev. Lett. 86 (2001) 2158.
[10] T. Kobayashi, T. Saito, H. Ohtani, Nature 414 (2001) 531.
[11] G. Lanzani, G. Cerullo, S. Stagira, M. Zavelani-Rossi, S. De Silvestri, Synth. Met. 119 (2001) 491.
[12] S. Adachi, V.M. Kobryanskii, T. Kobayashi, Phys. Rev. Lett. 89 (2002) 27401.
[13] N. Ishii, E. Tokunaga, S. Adachi, T. Kimura, H. Matsuda, T. Kobayashi, Phys. Rev. A 70 (2004) 023811.
[14] Y. Yuasa, M. Ikuta, T. Kobayashi, T. Kimura, H. Matsuda, Phys. Rev. B 72 (2005) 134302.
[15] T. Kobayashi, H. Wang, Z. Wang, T. Otsubo, J. Chem. Phys. 125 (2006) 044103.
[16] Z. Wang, T. Otsubo, T. Kobayashi, Chem. Phys. Lett. 430 (2006) 45.
[17] T. Kobayashi, A. Yabushita, T. Saito, H. Ohtani, M. Tsuda, Photochem. Photobiol. 83 (2007) 363.
[18] W.T. Pollard, S.Y. Lee, R.A. Mathies, J. Chem. Phys. 92 (1990) 4012.
[19] W.T. Pollard, S.L. Dexheimer, Q. Wang, L.A. Peteanu, C.V. Shank, R.A. Mathies, J. Phys. Chem. 96 (1992) 6147.
[20] I. Iwakura, A. Yabushita, T. Kobayashi, Chem. Phys. Lett. 457 (2008) 421.
[21] P. Vöhringer, D.C. Arnett, T.S. Yang, N.F. Scherer, Chem. Phys. Lett. 237 (1995) 387.
[22] P. Vöhringer, D.C. Arnett, R.A. Westervelt, M.J. Feldstein, N.F. Scherer, J. Chem. Phys. 102 (1995) 4027.
[23] P. Cong, Y.J. Yan, H.P. Deuel, J.D. Simon, J. Chem. Phys. 100 (1994) 7855.
[24] P. Vöhringer, R.A. Westervelt, T.S. Yang, D.C. Arnett, M.J. Feldstein, N.F. Scherer, J. Raman Spectrosc. 26 (1995) 535.
[25] I. Martini, G.V. Hartland, Chem. Phys. Lett. 258 (1996) 180.
[26] I. Martini, G.V. Hartland, J. Phys. Chem. 100 (1996) 19764.
[27] T.S. Yang et al., J. Chem. Phys. 110 (1999) 12070.
[28] T. Wilhelm, J. Piel, E. Riedle, Opt. Lett. 22 (1997) 1494.
[29] G. Cerullo, M. Nisoli, S. De Silvestri, Appl. Phys. Lett. 71 (1997) 3616.
[30] A. Shirakawa, I. Sakane, M. Takasaka, T. Kobayashi, Appl. Phys. Lett. 74 (1999) 2268.
[31] A. Baltuska, T. Fuji, T. Kobayashi, Opt. Lett. 27 (2002) 306.
[32] A.D. Becke, J. Chem. Phys. 98 (1993) 5648.
[33] C. Lee, W. Yang, R.G. Parr, Phys. Rev. B 37 (1988) 785.
[34] M.J. Frisch et al., Gaussian 03, Revision D.02 Gaussian Inc., Wallingford CT, 2004.
[35] A.N. Kumar, F. Rosca, A. Widom, P.M. Champion, J. Chem. Phys. 144 (2001) 701.